Dynamic Tire Friction Models for Vehicle Traction Control

Carlos Canudas de Wit[1]
Laboratoire d'Automatique de Grenoble, UMR CNRS 5528
ENSIEG-INPG, B.P. 46, 38 402 ST. Martin d'Heres, FRANCE

Panagiotis Tsiotras[2]
School of Aerospace Engineering
Georgia Institute of Technology, Atlanta, GA 30332-0150, USA

Abstract

In this paper we derive a dynamic friction force model for road/tire interaction for ground vehicles. The model is based on a similar dynamic friction model for contact developed previously for contact-point friction problems, called the LuGre model [4]. We show that the dynamic LuGre friction model is able to accurately capture velocity and road/surface dependence of the tire friction force.

1 Introduction

The problem of traction control for ground vehicles is of enormous importance to automotive industry. Traction control systems reduce or eliminate excessive slipping or sliding during vehicle acceleration and thus enhance the controllability and maneuverability of the vehicle. Proper traction control design will have a paramount effect on safety and handling qualities for future passenger vehicles. Traction control aims to achieve maximum torque transfer from the wheel axle to forward acceleration. The friction force in the tire/road interface is the main mechanism for converting wheel angular acceleration (due to the motor torque) to forward acceleration (longitudinal force). Therefore, the study of friction force characteristics at the road/tire interface has received a great deal of attention in the automotive literature.

A common assumption in most of tire friction models is that the normalized tire friction μ

$$\mu = \frac{F}{F_n} = \frac{\text{Friction force}}{\text{Normal force}}$$

is a nonlinear function of the normalized relative velocity between the road and the tire (slip coefficient s) with a distinct maximum; see Fig. 1. It is also understood that μ depends also on the velocity of the vehicle and road surface conditions, among other factors (see [3] and [10]). The curves shown in Fig. 1 illustrate how these factors influence the shape of μ.

[1]Directeur de Recherche. Corresponding author. Email: canudas@lag.ensieg.inpg.fr
[2]Associate Professor. Email: p.tsiotras@ae.gatech.edu

The static model shown in Fig. 1 is derived empirically based solely on steady-state experimental data [10, 1]. Under steady-state conditions, experimental data seem to support the force vs. slip curves of Fig. 1. Nevertheless, the development of friction force at the tire/road interface is very much a dynamic phenomenon. In other words, the friction force does not reach its steady-state instantaneously, but rather exhibits significant transient behavior which may differ significantly from its steady-state value. Experiments performed in commercial vehicles, have shown that the tire/road forces do not vary along the curves shown Fig. 1, but "jump" from one value to an other when these forces are displayed in the $\mu - s$ plane [15].

In this paper, we develop new, speed-dependent, dynamic friction models that can be used to describe the tire/road interaction. These models have the advantage that are developed starting from first principles and are based on simple contact (punctual) dynamic friction models [4]. Thus, the parameters entering the models have a physical significance which allows the designer to tune the model parameters based on experimental data. The models are also speed-dependent, which agrees with experimental observations. A simple parameter in the model can also be used to capture the road surface characteristics. Finally, our model is shown to be well-defined everywhere and hence, is appropriate for control law design.

2 Tire/road friction models

In this study we consider a system of the form:

$$m\dot{v} = F \quad (1)$$
$$J\dot{\omega} = -rF + u\,, \quad (2)$$

where m is 1/4 of the vehicle mass and J, r are the inertia and radius of the wheel, respectively. v is the linear velocity, ω is the angular velocity, u is the accelerating (or braking) torque, and F is the tire/road friction force. For the sake of simplicity, only longitudinal motion will be considered. The dynamics of the braking and driving actuators are also neglected.

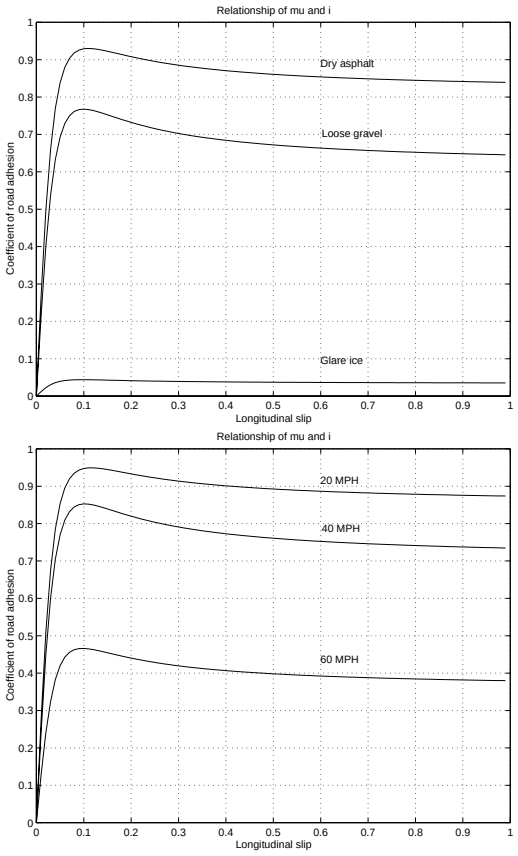

Figure 1: Typical variations of the tire/road friction profiles for: different road surface conditions (top), different vehicle velocities (bottom). Curves obtained by Harned in *et al* [10].

2.1 Slip/Force maps

The most common tire friction models used in the literature are those of slip/force maps. They are defined as one-to-one (memory-less) maps between the friction F, and the longitudinal slip rate s, defined as:

$$s = \begin{cases} 1 - \frac{r\omega}{v} & \text{if} \quad v > r\omega, v \neq 0 \quad \text{braking} \\ 1 - \frac{v}{r\omega} & \text{if} \quad v < r\omega, \omega \neq 0 \quad \text{driving} \end{cases} \tag{3}$$

The slip rate results from the reduction of the effective circumference of the tire (consequence of the tread deformation due to the elasticity of the tire rubber), which implies that the ground velocity will not be equal to $v = r\omega$. The slip rate is defined in the interval $[0, 1]$. When $s = 0$ there is no sliding (pure rolling), whereas $s = 1$ indicates full sliding.

The slip/force models aim at describing the shapes shown in Fig. 1 via static maps $F(s) : s \mapsto F$. They may also depend on the vehicle velocity v, i.e. $F(s, v)$, and vary when the road characteristics change.

One of the most well-known models of this type is Pacejka's model (see, Pacejka and Sharp [13]), also known as the "magic formula". This model has been shown to suitably match experimental data, obtained under particular conditions of constant linear and angular velocity. The Pacejka model has the form

$$F(s) = c_1 \sin(c_2 \arctan(c_3 s - c_4(c_3 s - \arctan(c_3 s)))) \,,$$

where the $c_i's$ are the parameters characterizing this model. These parameters can be identified by matching experimental data, as shown in Bakker *et al.* [1]. The parameters c_i depend on the tire characteristics (such as compound, tread type, tread depth, inflation pressure, temperature), on the road conditions (such as type of surface, texture, drainage, capacity, temperature, lubricant, i.e., water or snow), and on the vehicle operational conditions (velocity, load); see Pasterkamp and Pacejka [12].

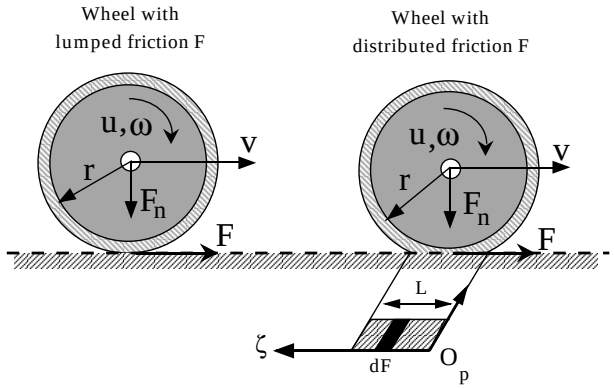

Figure 2: One-wheel system with: lumped friction (left), distributed friction (right)

As an alternative to the static $F(s)$ maps, dynamic models based on the dynamic friction models of Dahl [7][1], can be adapted to suitably describe the road-tire contact friction. Dynamic models can be formulated as a lumped or distributed models, as shown in Fig. 2. This distinction will be discussed next.

2.2 Lumped models

A lumped friction model assumes punctual tire-road friction contact. An example of such a model can be derived from the LuGre model[2] (see Canudas *et al*, [4]), i.e.

$$\dot{z} = v_r - \frac{\sigma_0 |v_r|}{g(v_r)} z \tag{4}$$

$$F = (\sigma_0 z + \sigma_1 \dot{z} + \sigma_2 v_r) F_n \tag{5}$$

with,

$$g(v_r) = \mu_C + (\mu_S - \mu_C) e^{-|v_r/v_s|^{\frac{1}{2}}}$$

[1] Dahl's models lead to a friction displacement relation that bears much resemblance with stress-strain relations proposed in classical solid mechanics.

[2] This model differs from the one in [4] in the way that the function $g(v)$ is defined. Here we propose to use the term $e^{-|v_r/v_s|^{\frac{1}{2}}}$ instead the term $e^{-(v_r/v_s)^2}$ as in the LuGre model in order to better match the pseudo-stationary characteristic of this model (map $s \mapsto F(s)$) with the shape of the Pacejka's model, as it will be shown later.

where σ_0 is the normalized rubber longitudinal lumped stiffness, σ_1 the normalized rubber longitudinal lumped damping, σ_2 the normalized viscous relative damping, μ_C the normalized Coulomb friction, μ_S the normalized Static friction,($\mu_C \leq \mu_S \in [0,1]$), v_S the Stribeck relative velocity, F_n the normal force, $v_r = (r\omega - v)$ the relative velocity, and z the internal friction state.

Dynamic friction models specifically for tires have been reported in the work of Clover and Bernard [6], where they develop a differential equation for the slip coefficient, starting from a simple relationship of the relative reflections of the tire elements in the tire contact patch. They still use the semi-empirical static force/slip models, however, to compute the corresponding friction force. In that respect, such models can be best described as quasi-dynamic models.

2.3 Distributed models

Distributed models assume the existence of an area of contact (or patch) between the tire and the road, as shown in Fig. 2. This patch represents the projection of the part of the tire that is in contact with the road. The contact patch is associated to the frame O_p, with ζ as the axis coordinate. The patch length is L.

Distributed dynamical models, have been studied previously, for example, in the works of Bliman *et al.* [2]. In these kinds of models, the contact patch area is discretized to a series of elements, and the microscopic deformation effects are studied in detail. In particular, Bliman *at al.* characterize the elastic and Coulomb friction forces at each point of the contact patch, but then they give the aggregate effect of these distributed forces by integrating over the whole patch area. They propose a second order rate-independent model (similar to Dahl's model), and show that, under constant v and ω, there exist a choice of parameters that closely match a curve similar to the one characterizing the magic formula.

Similar results can be obtained by using a model based in the first-order LuGre friction model, i.e.

$$\frac{d\,\delta z}{dt}(\zeta,t) = v_r - \frac{\sigma_0|v_r|}{g(v_r)}\,\delta z \tag{6}$$

$$F = \int_0^L \delta F(\zeta,t)\,d\zeta\,, \tag{7}$$

with $g(v_r)$ defined as before and

$$\delta F = (\sigma_0\,\delta z + \sigma_1\,\delta\dot{z} + \sigma_2 v_r)\,\delta F_n\,,$$

where, δF is the differential friction force, $\delta F_n = F_n/L$ the differential normal force, $v_r = (r\omega - v)$ the relative velocity, and δz the differential internal friction state. This model assumes that:

- the normal force is uniformly distributed, and
- the contact velocity of each differential state element is equal to v_r.

Nevertheless, it is also possible to include different normal force distribution if necessary, i.e. $\delta F_n = f(\zeta)$.

Note that Eq. (6) describes a partial differential equation (PDE), i.e.

$$\frac{d\,\delta z}{dt}(\zeta,t) = \frac{\partial\,\delta z}{\partial\zeta}(\zeta,t)\,r\omega + \frac{\partial\,\delta z}{\partial t}(\zeta,t) = v_r - \frac{\sigma_0|v_r|}{g(v_r)}\,\delta z \tag{8}$$

that should be solved in both: time and space.

2.4 Relation between distributed model and the magic formula

The linear motion of the differential δF in the patch frame O_p is $\dot{\zeta} = r\omega$, for positive ω, and $\dot{\zeta} = -r\omega$, for negative ω (the frame origin changes location when the wheel velocity reverses). Hence $\dot{\zeta} = r|\omega|$. We can thus rewrite (6) in the ζ coordinates as:

$$\frac{d\,\delta z}{d\zeta} = -\frac{\sigma_0|s|}{g(v_r)}\delta z + |s|\,\mathrm{sgn}(r\omega - v) \tag{9}$$

where $s = v_r/\omega r = 1 - v/\omega r$. Assuming that v, and ω are constant (hence also v_r, and s), the above equation describes a linear space-invariant system having the sign of the relative velocity as its input.

The solution of the above equation over the space interval $[\zeta(t_0),\zeta(t_1)]$, or equivalent over $[\zeta_0,\zeta_1]$, with $\delta z(\zeta_0) = \zeta_0 = 0$ is

$$\delta z(\zeta) = \mathrm{sgn}(v_r)\frac{g(v_r)}{\sigma_0}\left(1 - e^{-\frac{\sigma_0|s|}{g(v_r)}\zeta}\right)$$

Introducing this solution together with Eq. (9) in Eq. (7), and integrating, we obtain

$$\int_0^L \delta z(\zeta)\,d\zeta = \mathrm{sgn}(v_r)\frac{g(v_r)}{\sigma_0}L\left(1 + \frac{g(v_r)}{\sigma_0 L|s|}(e^{-\frac{\sigma_0 L|s|}{g(v_r)}} - 1)\right) \tag{10}$$

and using (8) we obtain

$$\int_0^L \delta\dot{z}(\zeta)\,d\zeta = -v_r\frac{g(v_r)}{\sigma_0|s|}(e^{-\frac{\sigma_0 L|s|}{g(v_r)}} - 1) \tag{11}$$

Finally, we have that $F(s)$, is given as

$$F(s) = \mathrm{sgn}(v_r)F_n g(s)\left(1 + \gamma\,\frac{g(s)}{\sigma_0 L|s|}(e^{-\frac{\sigma_0 L|s|}{g(s)}} - 1)\right) + F_n\sigma_2 r\omega s \tag{12}$$

with $\gamma = 1 - \sigma_1|v_r|/g(s)$ and

$$g(s) = \mu_C + (\mu_S - \mu_C)\,e^{-|r\omega s/v_s|^{\frac{1}{2}}}$$

for some constant ω, and $s \in [0,1]$.

Uncertainty in the knowledge of the function $g(v_r)$, can be modeled by introducing the parameter θ, as

$$\tilde{g}(v_r) = \theta g(v_r)\,,$$

where $g(v_r)$ is the nominal known function. Computation of the function $F(s,\theta)$, from Eq. (12) as a function

Parameter	Value	Units
σ_0	40	[1/m]
σ_1	4.9487	[s/m]
σ_2	0.0018	[s/m]
μ_C	0.5	[-]
μ_S	0.9	[-]
v_s	12.5	[m/s]

Table 1: Data used for the plot shown in Fig. 3

of θ, gives the curves shown in Fig. 3. These curves match reasonably well the experimental data shown in Fig. 1-(a), for different coefficient of road adhesion using the parameters shown in Table 1. Hence, the parameter θ, suitably describes the changes in the road characteristics.

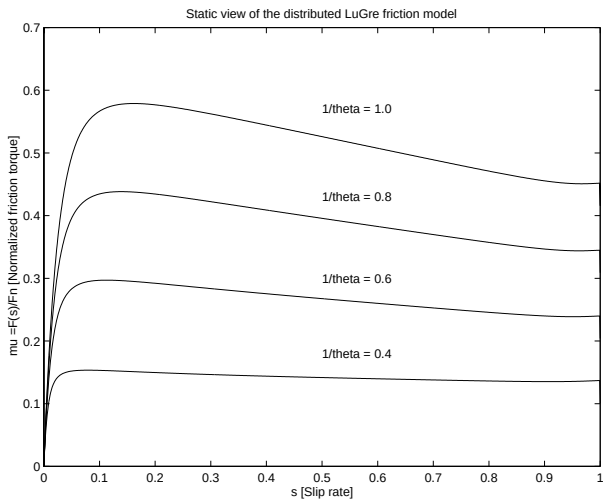

Figure 3: Static view of the distributed LuGre model, under different values for $1/\theta$. Braking case, with $v = 20m/s = 72Km/h$. These curves show the normalized friction $\mu = F(s)/F_n$, as a function of the slip rate s.

Note that the steady-state representation of Eq. (12) can be used to identify the model parameters by feeding this model to experimental data. These parameters can also be used in the simpler lumped model, which can be shown to suitably approximate the solution of the PDE described by Eqs. (6) and (7). This approximation is discussed next.

2.5 From distributed to lumped models

Under the assumptions given in subsection 2.3 we can approximate the PDE in Eqs. (6)-(7) by a set of n ordinary differential equations via a spatial discretization. To this end, let's divide the contact patch into N equally spaced discrete points, to each we associate the "discrete" average displacement δz_i, i.e. $\delta z_i = \delta z(iL/N, t),\ \forall i = 0, 1, \ldots N-1$. The space/time scalar $\delta z(\zeta, t)$ is thus approximated by the N-dimensional time vector, $\delta z = [\delta z_0, \delta z_1, \ldots, \delta z_{N-1}]^T$ where, for the sake of simplicity of the notation, we have written $\delta z_i(t) = \delta z_i$. Similarly, we have that

$$\frac{d\,\delta z}{d\zeta} = [\frac{d\,\delta z_0}{d\zeta}, \frac{d\,\delta z_1}{d\zeta}, \ldots \frac{d\,\delta z_{N-1}}{d\zeta}]^T \tag{13}$$

where each of the $\frac{d\,\delta z_i}{d\zeta}$ can be approximated using forward differences, as:

$$\frac{d\,\delta z_i}{d\zeta} = \begin{cases} \frac{\delta z_{i+1} - \delta z_i}{L/N} & i = 0, 1, \ldots N-2 \\ 0 & i = N-1 \end{cases}$$

Hence, for each i-th equation we have

$$\delta \dot{z}_i = -\frac{\delta z_{i+1} - \delta z_i}{L/N} r\omega + v_r - \sigma_0 \frac{|v_r|}{g(v_r)} \delta z_i \tag{14}$$

Similarly,with $\Delta F_{n,i} = F_n/L,\ \forall\, i$, and $\Delta\zeta = L/N$, F can be approximated as:

$$F = \sum_{i=0}^{N-1} \Delta F_i = \sum_{i=0}^{N-1} (\sigma_0\, \delta z_i + \sigma_1\, \delta \dot{z}_i)\, \Delta F_{n,i} \Delta\zeta + \sigma_2 v_r F_n$$

which simplifies to:

$$F = F_n \frac{1}{N} \sum_{i=0}^{N-1} (\sigma_0\, \delta z_i + \sigma_1\, \delta \dot{z}_i) + \sigma_2 v_r F_n$$

Introducing $\bar{z}$, as the mean value of all the δz_i, i.e.

$$\bar{z} = \frac{1}{N} \sum_{i=0}^{N-1} \delta z_i$$

we have, from Eq. (14), that

$$\dot{\bar{z}} = -\frac{1}{L} \sum_{i=0}^{N-1} (\delta z_{i+1} - \delta z_i)\, r\omega + v_r - \sigma_0 \frac{|v_r|}{g(v_r)} \delta \bar{z} \tag{15}$$

Noticing that $\sum_{i=0}^{N-1} (\delta z_{i+1} - \delta z_i) = \delta z_0$, and taking $\delta z_0 = 0$, we have that

$$\dot{\bar{z}} = v_r - \frac{\sigma_0 |v_r|}{g(v_r)} \bar{z} \tag{16}$$

$$F = (\sigma_0 \bar{z} + \sigma_1 \dot{\bar{z}} + \sigma_2 v_r)\, F_n \tag{17}$$

These equations describe the approximate behaviour of the PDE, in terms of the mean variable $\bar{z}$. When compared to Eqs. (4)-(5), they indicate that the lumped model can be used as a suitable approximation of the distributed one. Therefore, parameters identified from the stationary behaviour shown in Fig. 3, can be used in the lumped model (4)-(5).

3 Traction Control

We consider the one-wheel model with the tire/road friction described in Eqs. (1)-(2). Using the pseudo-static (or steady-state) force friction point of view, the friction force is given as an algebraic (static) function of

the slip coefficient. Typical friction force vs. slip coefficient curves are shown in Fig. 1. This figure suggests a simple way to achieve maximum traction between the road and the wheel tire. Namely, to operate at the maximum point of the friction/slip curve. This "extremum seeking" control strategy requires the *a priori* knowledge of the optimal target slip. With the exception of [8], where the authors present a control algorithm which does not require the *a priori* knowledge of the optimal slip, current literature does not seem to have adequately dealt with this problem. Nonetheless, slip and friction estimation algorithms have been proposed and verified experimentally in [12].

A simple traction control law using this idea, and based on sliding mode techniques, is given in [9]. For the simplified one-wheel friction model of Eqs. (1)-(2) this control law is given by

$$u = \left[\frac{J}{rm(1-s_d)} + r\right] F - k\,\mathrm{sgn}(S) \qquad (18)$$

where s_d is the desired slip coefficient, S is given by $S = (s - s_d)\, r\omega$ and

$$k = \frac{J}{(1-s_d)r}\,\eta, \qquad \eta > 0 \qquad (19)$$

Indeed, simple calculation shows that

$$\dot{S} = (1 - s_d)\, r\dot{\omega} - \dot{V} \qquad (20)$$

Substituting Eq. (18) into Eq. (20) and using Eqs. (1)-(2), one obtains

$$\dot{S} = -\eta\,\mathrm{sgn}(S) \qquad (21)$$

This implies that $S \to 0$ after $S(0)/\eta$ seconds. The major drawback of the control law in Eq. (18) is that is highly oscillatory due to the zero order sliding mode $S = 0$. One can reduce the chattering by smoothing the discontinuity of $\mathrm{sgn}(\cdot)$ via low-pass filtering. In the smoothed implementation of the previous control law, the term $k\,\mathrm{sgn}(S)$ is replaced by the term $\bar{k}\,\mathrm{sat}(S/\Phi)$, where $\bar{k} = \lambda\,\Phi$ and where $\mathrm{sat}(\cdot)$ is the saturation function. For more details on the previous control law, the interested reader is referred to [9].

4 Numerical example

In this section we use the traction control law of the previous section on two different friction models. In particular, we are interested in differences between static and dynamic friction models. We consider the one-wheel model with the values shown in Table 1, and: $m = 500\,Kg$, $J = 0.2344\,Kgm^2$, $r = 0.25\,m$, $F_n = mg$. The first simulation was performed using the steady-state LuGre model from Eq. (12). The relevant parameters of the LuGre friction model are shown in Table 1. The maximum traction is achieved for $s_d = 0.15$. The results of the simulations, using the smoothed version of the traction control law presented in the previous section, are shown in Fig. 4. The second simulation

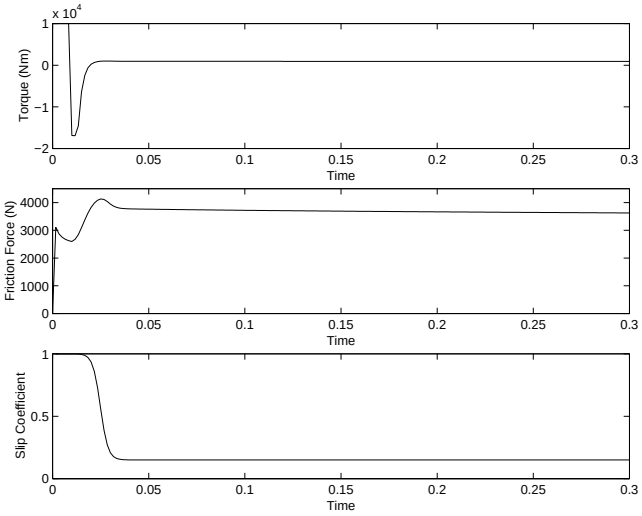

Figure 4: Static friction model.

was performed using the dynamic friction model given in Eqs. (4)-(5) with the values shown in Table 1. The results of the simulation are shown in Fig. 5. In both cases, the initial applied torque for both static and dynamic cases was $u = 10000Nm$. The history profiles of

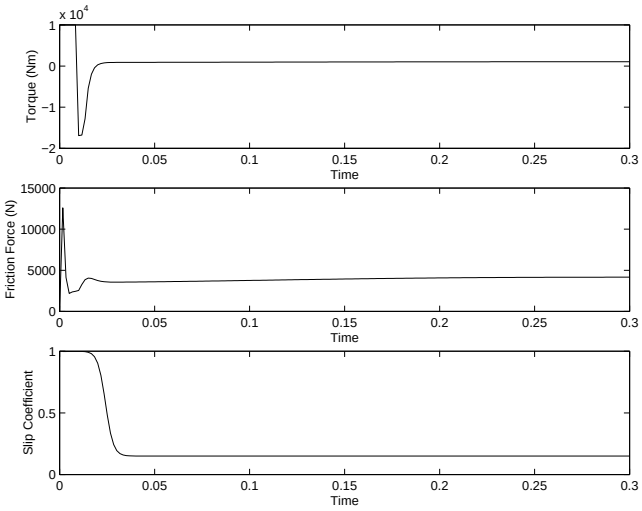

Figure 5: Dynamic friction model.

the applied torque and the slip coefficient are very similar. The most serious discrepancy between Figs. 4 and 5 is the actual friction force developed between the tire and the ground for the two cases. These figures show clearly that the maximum friction force predicted using the dynamic friction model is more than three times the maximum of the friction force predicted using the static friction model during the initial transient. The steady-state value of the friction force for both cases is almost the same. Since the main mechanism for transferring the axle torque to forward movement is friction force, these results suggest that new traction control algorithms using dynamic friction models may have an

advantage over traditional control laws based on tracking the optimal slip coefficient. Finally, Fig. 6 shows the distances traveled by the wheel for each case, along with the path of a point at the circumference of the wheel. A complete circle indicates complete slipping (the wheel spins without moving forward) whereas a cycloid indicates that the relative velocity of the contact point is zero. Because of the higher friction force developed in the dynamic friction model, the wheel has traveled a longer distance than for the static friction case.

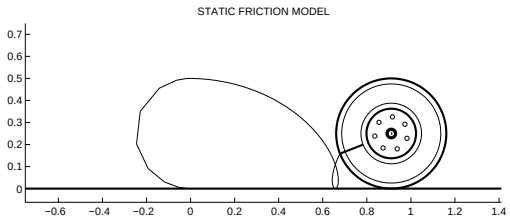

(a) Wheel trajectory with static friction model.

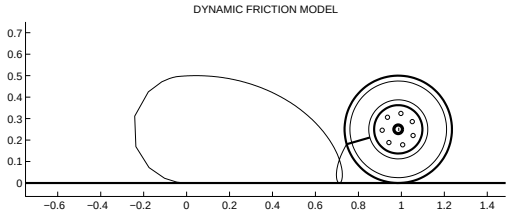

(b) Wheel trajectory with dynamic friction model.

Figure 6: Comparison of wheel trajectories using static and dynamic tire friction models (note different stopping points).

5 Conclusion

In this paper, we have derived a new dynamic, speed- and surface-dependent tire friction model for use in vehicle traction control design. This model captures very accurately most of the main characteristics that have been discovered via experimental data. It was also shown that distributed models can collapse to a lumped model, which is rich enough to capture the main dynamic characteristics. Since the main mechanism for transferring the axle torque to forward movement is friction force, these results suggest that new traction control algorithms using dynamic friction models may have an advantage over traditional control laws based on simple, static friction models. Although for the sake of brevity the discussion has been restricted to traction control, the results of the paper have an immediate application to the design of ABS systems.

Acknowledgements

The LuGre version of the dynamic friction model was developed during the visit of the first author at the School of Aerospace Engineering at the Georgia Institute of Technology during December 1998, as part of the CNRS/NSF collaboration project (NSF award no. INT-9726621/INT-9996096). The first author would like to thank M. Sorine and P.A. Bliman for interesting discussions on distributed friction models.

References

[1] Bakker, E., L. Nyborg, and H. Pacejka, "Tyre Modelling for Use in Vehicle Dynamic Studies," Society of Automotive Engineers Paper # 870421, 1987.

[2] Bliman, P.A., T. Bonald, and M. Sorine, "Hysteresis Operators and Tire Friction Models: Application to vehicle dynamic Simulator," *Prof. of ICIAM. 95*, Hamburg, Germany, 3-7 July, 1995.

[3] Burckhardt, M., *Fahrwerktechnik: Radschlupfregelsysteme.* Vogel-Verlag, Germany, 1993.

[4] Canudas de Wit, C., H. Olsson, K. J. Åström, and P. Lischinsky, "A New Model for Control of Systems with Friction," *IEEE TAC*, Vol. 40, No. 3, pp. 419-425, 1995.

[5] Canudas de Wit, C., R. Horowitz, R. and P. Tsiotras, "Model-Based Observers for Tire/Road Contact Friction Prediction," In *New Directions in Nonlinear Observer Design*, Nijmeijer, H. and T.I Fossen (Eds), Springer Verlag, Lectures Notes in Control and Information Science, May 1999.

[6] Clover, C. L. and J. E. Bernard, "Longitudinal Tire Dynamics," *Vehicle System Dynamics*, Vol. 29, pp. 231–259, 1998.

[7] Dahl, P. R., "Solid Friction Damping of Mechanical Vibrations," *AIAA Journal*, Vol. 14, No. 12, pp. 1675-1682, 1976.

[8] Drakunov, S., Ü. Özgüner, P. Dix, and B. Ashrafi, "ABS Control Using Optimum Search via Sliding Modes," *IEEE Transactions on Control Systems Technology*, Vol. 3, No. 1, pp. 79–85, 1995.

[9] Fan, Z., Y. Koren, and D. Wehe, A Simple Traction Control for Tracked Vehicles. In *Proceedings of the American Control Conference*, pp. 1176–1177, Seatlle, WA, 1995.

[10] Harned, J., L. Johnston, and G. Scharpf, Measurement of Tire Brake Force Characteristics as Related to Wheel Slip (Antilock) Control System Design. *SAE Transactions*, Vol. 78 (Paper # 690214), pp. 909–925. 1969.

[11] Liu, Y. and J. Sun, "Target Slip Tracking Using Gain-Scheduling for Antilock Braking Systems," In *The American Control Conference*, pp. 1178–82, Seattle, WA, 1995.

[12] Pasterkamp, W. R. and H. B. Pacejka, "The Tire as a Sensor to Estimate Friction," *Vehicle Systems Dynamics*, Vol. 29, pp. 409-422, 1997.

[13] Pacejka, H. B. and R. S. Sharp, "Shear Force Developments by Psneumatic tires in Steady-State Conditions: A Review of Modeling Aspects," *Vehicle Systems Dynamics*, Vol. 20, pp. 121-176, 1991.

[14] Wong J. Y., *Theory of Ground Vehicles.* John Wiley & Sons, Inc., New York, 1993.

[15] van Zanten, A., W. D. Ruf, and A. Lutz, "Measurement and Simulation of Transient Tire Forces," in *International Congress and Exposition*, (Detroit, MI). SAE Technical Paper # 890640, 1989.